High-Resolution Paleomonsoon Variability in the Core Monsoon Zone: Multi-Proxy Geochemical Evidence from Recent Holocene Sediments of Lonar Impact Crater Lake, Central India

M. M. Kasdekar[1], P.N. Chikhalkar[2], Y. K. Mawale[3]

P.G. Department of Geology, Sant Gadge Baba Amravati University (SGBAU), Amravati, Maharashtra 444 602, India

***Corresponding Author**

DOI: https://doi.org/10.51584/IJRIAS.2026.110100102

Received: 26 January 2026; Accepted: 31 January 2026; Published: 12 February 2026

ABSTRACT

The Indian Summer Monsoon (ISM) exhibits significant variability at multiple timescales, yet high-resolution paleoclimate records from the core monsoon zone capturing centennial-scale monsoon dynamics during climatically critical periods remain limited. This study presents X-Ray Fluorescence (XRF) and Inductively Coupled Plasma Mass Spectrometry (ICP-MS) geochemical analysis of a 55 cm post-monsoon sediment core collected from Lonar Lake, a meteorite impact crater lake in central India's core monsoon zone (19.97°N, 76.51°E). The core comprises subsamples analyzed for major elements and trace elements. Integration with published sedimentation rates (50–80 cm/ka) indicates the core represents 900–950 years of recent Holocene history spanning the Medieval Warm Period (~1050–1300 CE), Medieval Warm Period–Little Ice Age transition (~1300–1400 CE), Little Ice Age climax (~1400–1850 CE), and the modern period (~1850–2024 CE). Paleoclimate indices reveal: (1) stable moderate chemical weathering (Chemical Index of Alteration [CIA] = 59.05 ± 1.03) consistent with semi-arid to sub-humid monsoon climate; (2) anomalously elevated Al/Na ratios in the middle core section indicating intensified chemical weathering during the Little Ice Age, contrary to global cooling trends; (3) V/Cr minima and Co maxima in the same interval indicating episodic anoxic conditions and productivity surges linked to enhanced monsoon precipitation; and (4) progressive Ba depletion reflecting long-term evolution toward more oxidizing depositional conditions. These findings challenge simplified global cooling–monsoon suppression paradigms and underscore centennial-scale ISM variability during a climatically critical recent Holocene interval.

Keywords: Indian Summer Monsoon, paleoclimate reconstruction, X-Ray Fluorescence geochemistry, weathering indices, trace metal paleoproxies, Little Ice Age, Medieval Warm Period, impact crater lake.

INTRODUCTION

The Indian Summer Monsoon (ISM) is a critical component of the global climate system, profoundly affecting precipitation patterns, agriculture, and human societies across South Asia (Goswami et al., 2006). Monsoon intensity fluctuations at multiple timescales—seasonal, interannual, decadal, centennial, and millennial generate substantial climate variability in this region (Sinha et al., 2011). Understanding the natural variability of the monsoon system is essential for accurate climate modeling, paleoclimate reconstruction, and projecting future monsoon behavior under anthropogenic climate change (Anoop et al., 2013; Dani & Ramesh, 2015).

Lake sediment archives from the core monsoon zone represent exceptional repositories of ISM variability information, capturing precipitation-driven changes in sediment flux, chemical weathering intensity, depositional redox conditions, and aquatic productivity (Basavaiah et al., 2014). Lonar Lake, a meteorite impact crater lake located in Buldhana District, Maharashtra, has emerged as an exceptional paleoclimate archive (Prasad et al., 2014; Menzel et al., 2014). Previous studies identified prolonged drought intervals and connections between monsoon variability and Indo-Pacific warm pool dynamics (Prasad et al., 2014; Sarkar et al., 2015).

ISSN No. 2454-6194 | DOI: 10.51584/IJRIAS |Volume XI Issue I January 2026

However, research opportunities remain for high-resolution geochemical analysis of recent Holocene sediments to reveal centennial-scale dynamics during the Medieval Warm Period and Little Ice Age.

This study presents results from a 55 cm post-monsoon sediment core collected from Lonar Lake, analyzed using XRF and ICP-MS geochemistry. Our objectives are to establish chronostratigraphy, characterize paleoclimate signals through weathering indices (CIA, CIW, PIA), and document paleomonsoon variability during the Medieval Warm Period–Little Ice Age transition.

Regional Setting

Lonar Lake Crater Geology

Lonar Lake occupies a well-preserved impact crater in the Deccan Plateau, an extensive Late Cretaceous flood basalt province (~65 Ma) covering approximately 500,000 km² of peninsular India (Fredriksson et al., 1973; Chandran et al., 2022). The crater exhibits classic morphology with a diameter of ~1.8 km and a depth of 150 m (Komatsu et al., 2014). The target rocks are low-K tholeiitic basalts (Fredriksson et al., 1973). This geologically homogeneous basaltic composition ensures that geochemical variations in lake sediments reflect changes in weathering intensity rather than provenance shifts (Menzel et al., 2014).

Modern Climate and Hydrology

Located in the core monsoon zone, the region receives maximum southwest monsoon (SWM) precipitation. The climate is semi-arid to sub-humid with a mean annual temperature of 26–30°C and precipitation of 700–900 mm, 80–90% of which falls between June and September (Prasad et al., 2014; Resmi et al., 2022). The lake is an endorheic system, hyperalkaline (pH 9.5–10) and hypersaline, fed by the ephemeral Dhara rivulet and groundwater seeps (Komatsu et al., 2014).

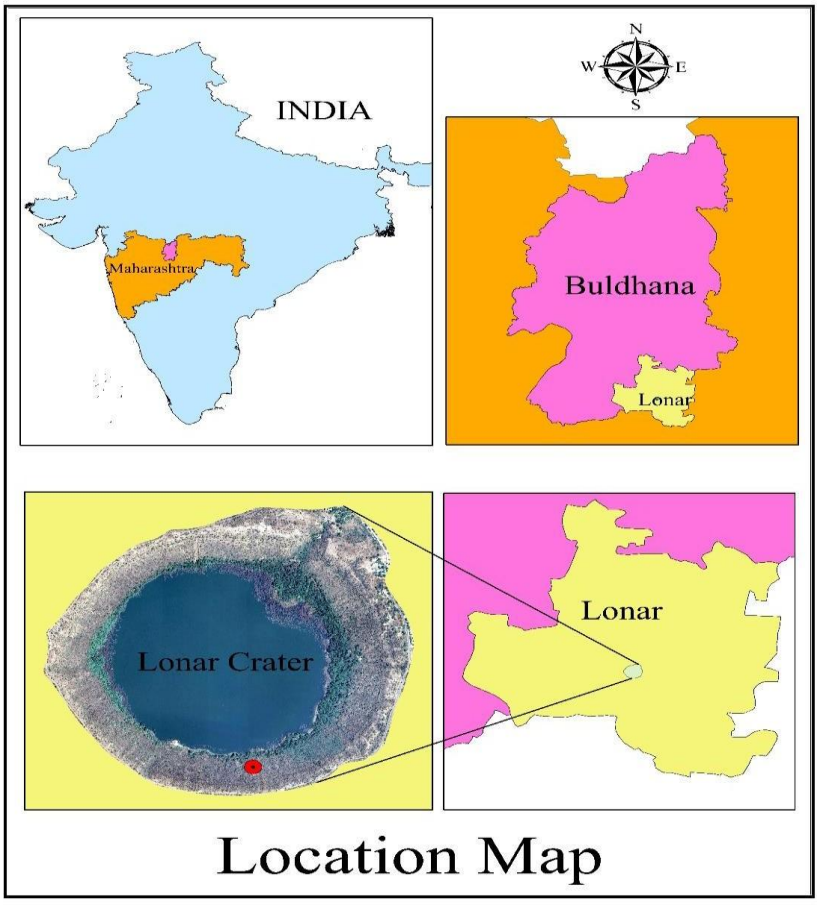

Figure 1 (A): Map of India showing the location of Lonar Lake in the core monsoon zone.

ISSN No. 2454-6194 | DOI: 10.51584/IJRIAS |Volume XI Issue I January 2026

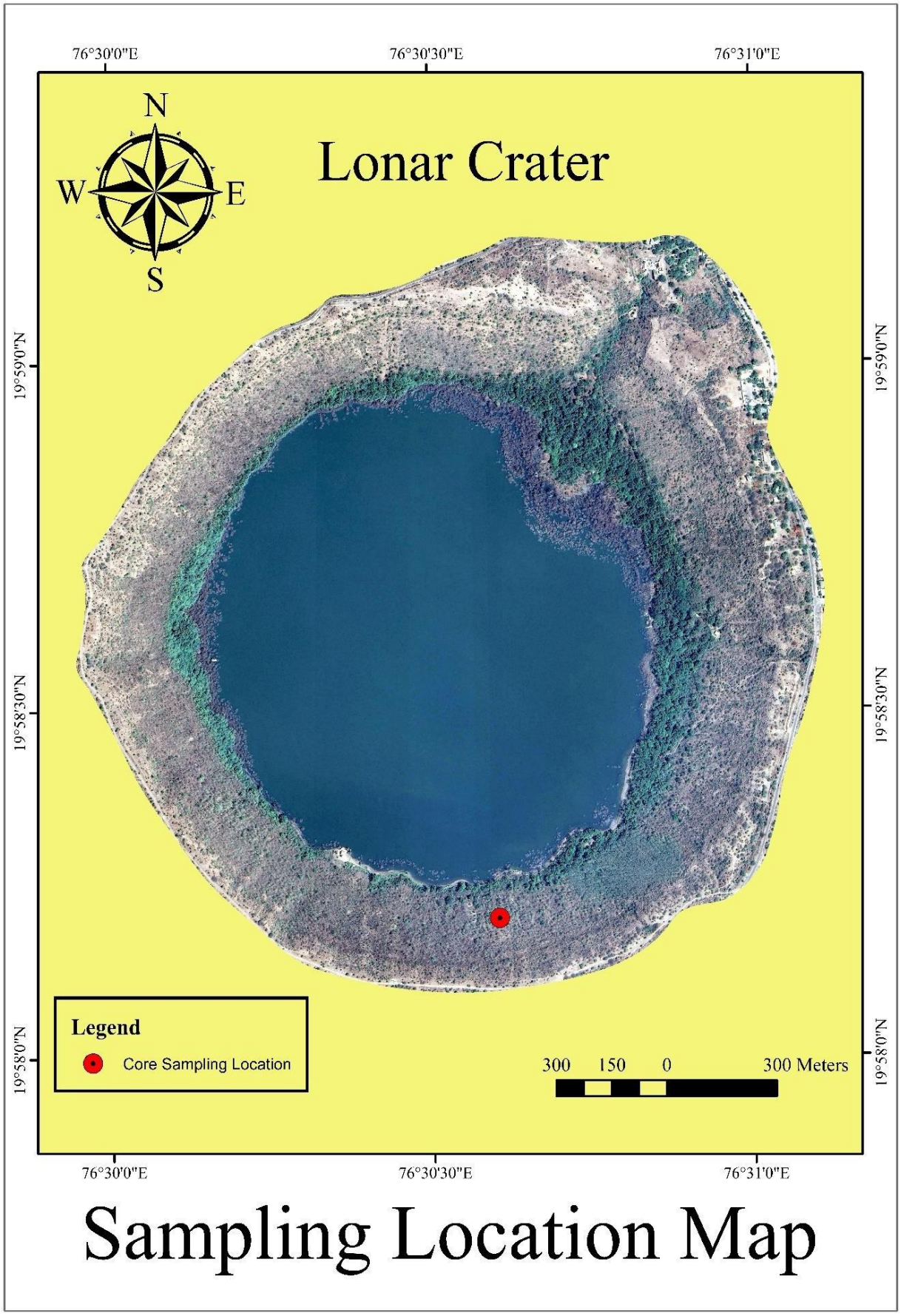

Figure 1 (B)*: Detailed map of Lonar Lake crater showing the main coring location (19.97°N, 76.51°E).*

ISSN No. 2454-6194 | DOI: 10.51584/IJRIAS |Volume XI Issue I January 2026

MATERIALS AND METHODS

Core Collection and Sampling

A 55 cm sediment core was recovered from the central lake basin (19.970779°N, 76.509170°E) using a gravity corer during the post-monsoon season (December 2024). The core was subsampled at approximately 2.2 cm intervals, generating samples L1 (bottom, 55 cm) to L25 (top, 0 cm). A surface sediment sample (L125) was collected from an adjacent location.

Analytical Methods

Samples were analyzed at the Wadia Institute of Himalayan Geology (WIHG), New Delhi.

- **Major Elements (XRF):** Determined as weight percent oxides (Na_2O, MgO, Al_2O_3, SiO_2, P_2O_5, K_2O, CaO, TiO_2, MnO, Fe_2O_3) and Loss-on-Ignition (LOI) at 110°C and 1000°C (Armstrong-Altrin & Verma, 2005).
- **Trace Elements (ICP-MS):** Determined in parts per million (ppm), including Ba, Cr, V, Sc, Co, Ni, Cu, Zn, Ga, Pb, Rb, Sr, Y, Zr, Nb, Th, and U.
- **Precision:** Estimated at ±2% RSD for major elements and ±5% RSD for trace elements.

Paleoclimate Indices

The Chemical Index of Alteration (CIA) was calculated following Nesbitt and Young (1982):

$$CIA = [Al_2O_3/ (Al_2O_3 + CaO^* + Na_2O + K_2O)] *100$$

where CaO* represents CaO in the silicate fraction. Supplementary indices included the Chemical Index of Weathering (CIW) and Plagioclase Index of Alteration (PIA) (Harnois, 1988; Fedo et al., 1995).

Chronology

In the absence of direct radiometric dating, an age-depth model was constructed using published sedimentation rates of 50–80 cm/ka (Prasad et al., 2014; Sarkar et al., 2015). Using an average rate of ~60 cm/ka, the base of the core (55 cm) is estimated at ~950 years BP (~1050 CE).

RESULTS

Core Chronostratigraphy

The estimated chronology places the core base (L1) in the Medieval Warm Period and the core top (L25) in the modern era.

Table 1 :Estimated Chronostratigraphy and Paleoclimate Phases

Sample	Depth (cm)	Est. Age (BP)	Est.Calendar Age	Paleoclimate Phase
L1	55	~950	~1050 CE	Medieval Warm Period
L9	35	~768	~1232 CE	MWP–LIA Transition
L13	27.5	~636	~1364 CE	Little Ice Age Climax
L25	0	~45	~1975 CE	Modern Period

ISSN No. 2454-6194 | DOI: 10.51584/IJRIAS |Volume XI Issue I January 2026

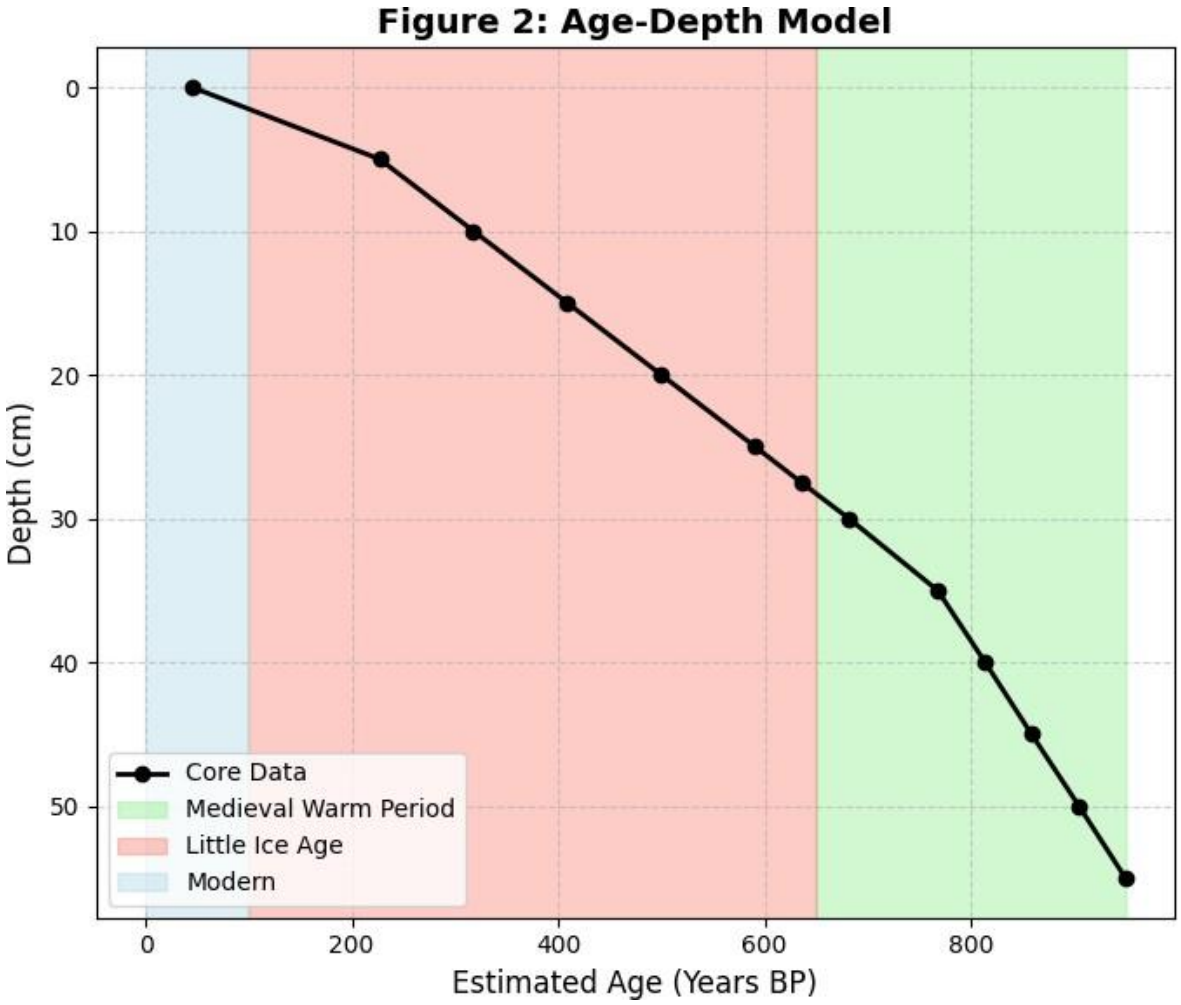

Figure 2: Sediment core stratigraphy showing sample positions and paleoclimate periods (Medieval Warm Period, Little Ice Age, Modern).

Geochemical Composition

Major element concentrations show high silica (mean 54.47%) and aluminum (mean 12.72%) uniformity, confirming basaltic provenance. Trace element data reveals significant variability in redox-sensitive elements (V, Cr, Co) and productivity proxies (Ba). The complete geochemical dataset is presented in Tables 2 and 3.

Table 2:Major Element Geochemistry (Weight % Oxides)

Sample	Na_2O	MgO	Al_2O_3	SiO_2	P_2O_5	K_2O	CaO	TiO_2	MnO	Fe_2O_3	Sum	LOI
L1	2.83	3.60	12.90	53.93	0.20	0.43	6.56	2.01	0.17	12.95	95.58	7.06
L3	2.67	3.63	12.71	54.85	0.20	0.41	6.25	2.03	0.17	13.07	95.99	8.22
L5	2.59	3.61	12.48	54.90	0.19	0.41	6.05	2.01	0.15	13.10	95.49	9.15
L7	2.54	3.61	12.52	54.67	0.18	0.40	6.16	2.08	0.16	13.25	95.57	9.42
L9	2.48	3.69	12.80	55.40	0.18	0.37	6.21	2.19	0.16	13.52	97.00	8.38
L11	2.49	3.67	12.92	55.33	0.19	0.37	6.38	2.19	0.17	13.30	97.01	7.79
L13	2.45	3.65	12.93	55.24	0.19	0.37	6.38	2.22	0.17	13.29	96.89	7.73

L15	2.47	3.65	12.97	55.07	0.19	0.38	6.50	2.29	0.17	13.37	97.06	6.81
L17	2.53	3.77	12.89	54.32	0.22	0.44	6.73	2.39	0.17	13.54	97.00	6.37
L19	2.53	3.74	12.94	54.67	0.21	0.42	6.74	2.55	0.18	13.76	97.74	6.42
L21	2.57	3.77	12.75	54.85	0.21	0.42	6.73	2.56	0.18	13.90	97.94	6.44
L23	2.54	3.84	12.47	54.14	0.20	0.42	6.71	2.69	0.18	14.02	97.21	6.55
L25	2.72	3.67	12.90	53.47	0.22	0.47	6.86	2.42	0.18	13.63	96.54	5.43

Table 3: Trace Element Geochemistry (PPM)

Sample	**Ba**	**Cr**	**V**	**Sc**	**Co**	**Ni**	**Cu**	**Zn**	**Pb**	**Th**	**Rb**	**Sr**	**Y**	**Zr**
L1	39	76	288	23	101	35	134	113	10	0.7	179	18	114	10
L3	39	110	290	23	74	37	144	118	12	1.5	188	20	117	10
L5	43	108	290	24	77	37	150	117	12	0.9	187	19	115	10
L7	40	92	286	24	79	37	151	120	12	BDL	187	19	118	10
L9	29	110	303	24	87	38	157	125	11	BDL	184	19	117	11
L11	27	123	302	24	75	38	149	121	13	BDL	184	19	113	10
L13	27	129	302	24	79	37	149	121	10	BDL	183	19	113	10
L15	19	97	314	24	91	35	148	124	10	1.2	179	18	112	10
L17	14	95	314	25	84	34	143	126	10	1.1	174	18	111	10
L19	13	109	320	24	80	36	145	128	11	BDL	171	17	110	11
L21	12	112	323	24	**136**	35	151	131	11	1.6	169	17	110	9
L23	8	94	329	25	**132**	36	149	135	10	BDL	170	17	110	11
L25	10	89	319	23	85	36	144	128	13	BDL	174	17	110	11

Paleoclimate Proxies

- **Weathering:** CIA values average 59.05 ± 1.03, indicating stable semi-arid to sub-humid conditions.
- **Al/Na Ratio:** Elevated values (up to 5.26) appear in the middle core section (samples 11–19).
- **Redox Conditions:** The V/Cr ratio shows minima (strongly reducing) in samples 13–19.
- **Productivity:** Cobalt (Co) peaks at 136 ppm in sample 21, coinciding with reducing signals.
- **Barium:** A systematic depletion from 39 ppm (L1) to 10 ppm (L25) is observed, with sample L125 showing a return to 39 ppm, likely due to surface anomalies.

ISSN No. 2454-6194 | DOI: 10.51584/IJRIAS |Volume XI Issue I January 2026

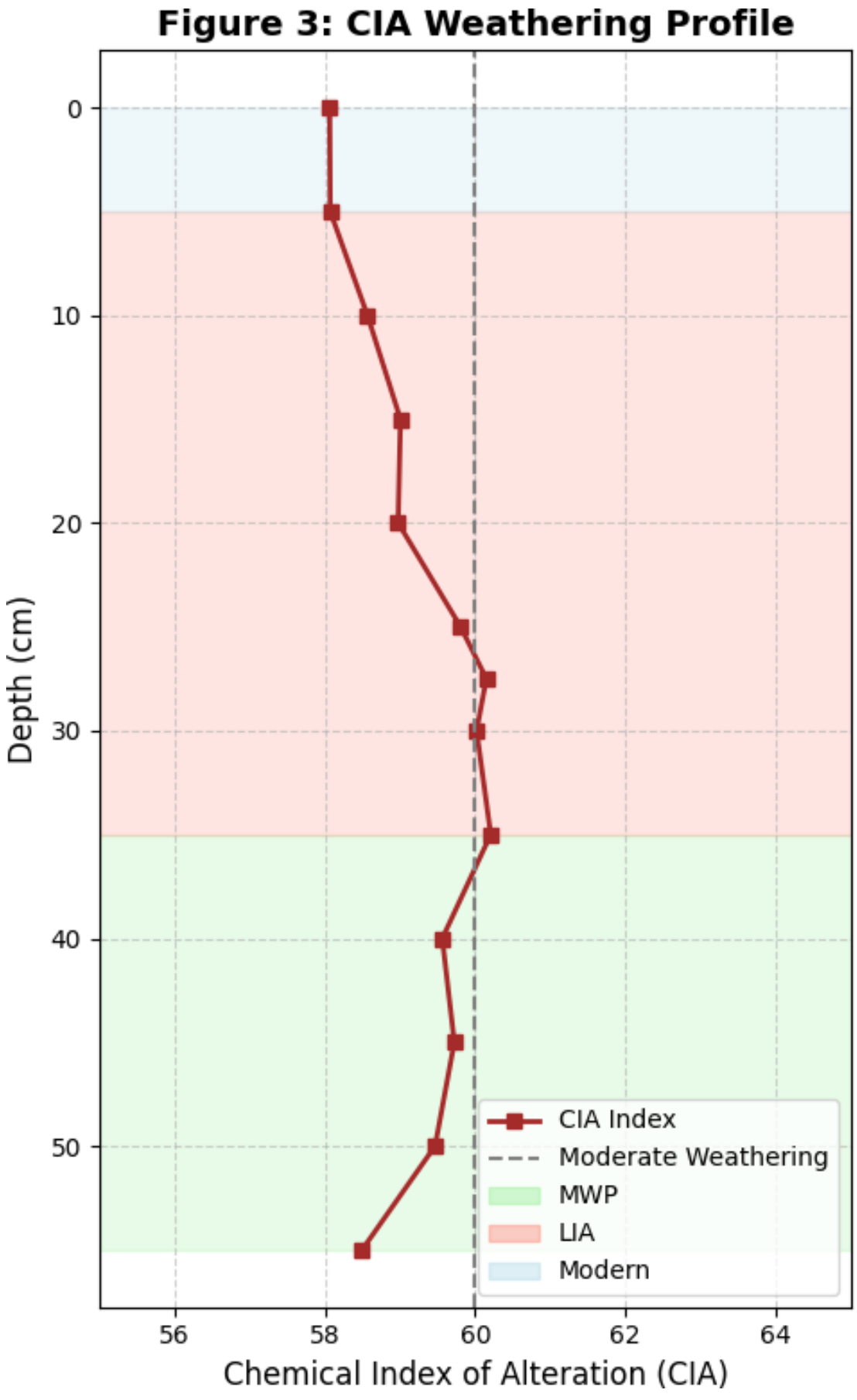

Figure 3: Stratigraphic variation of chemical weathering indices and trace element ratios through the 55 cm sediment core. Note the stability of CIA contrasted with the variability in redox proxies.

ISSN No. 2454-6194 | DOI: 10.51584/IJRIAS |Volume XI Issue I January 2026

Figure 4: Multi-Proxy Geochemical Record

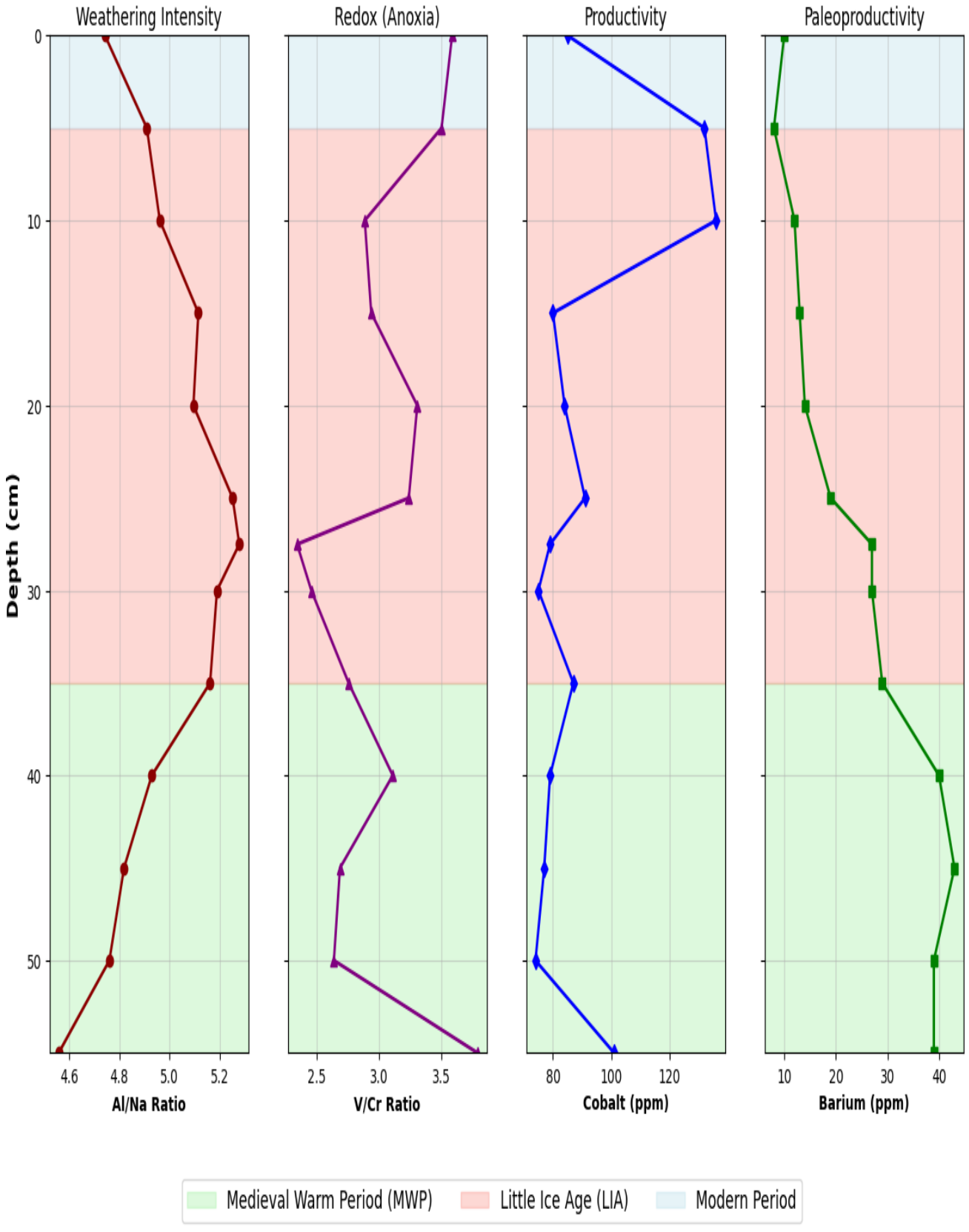

Figure 4 : Multi-proxy geochemical record showing the "Little Ice Age Paradox." Note the convergence of elevated Al/Na ratios (intensified weathering) and Cobalt/V/Cr peaks (anoxia and productivity) during

ISSN No. 2454-6194 | DOI: 10.51584/IJRIAS |Volume XI Issue I January 2026

the Little Ice Age band (shaded red), indicating episodic monsoon intensification during a globally cool period.

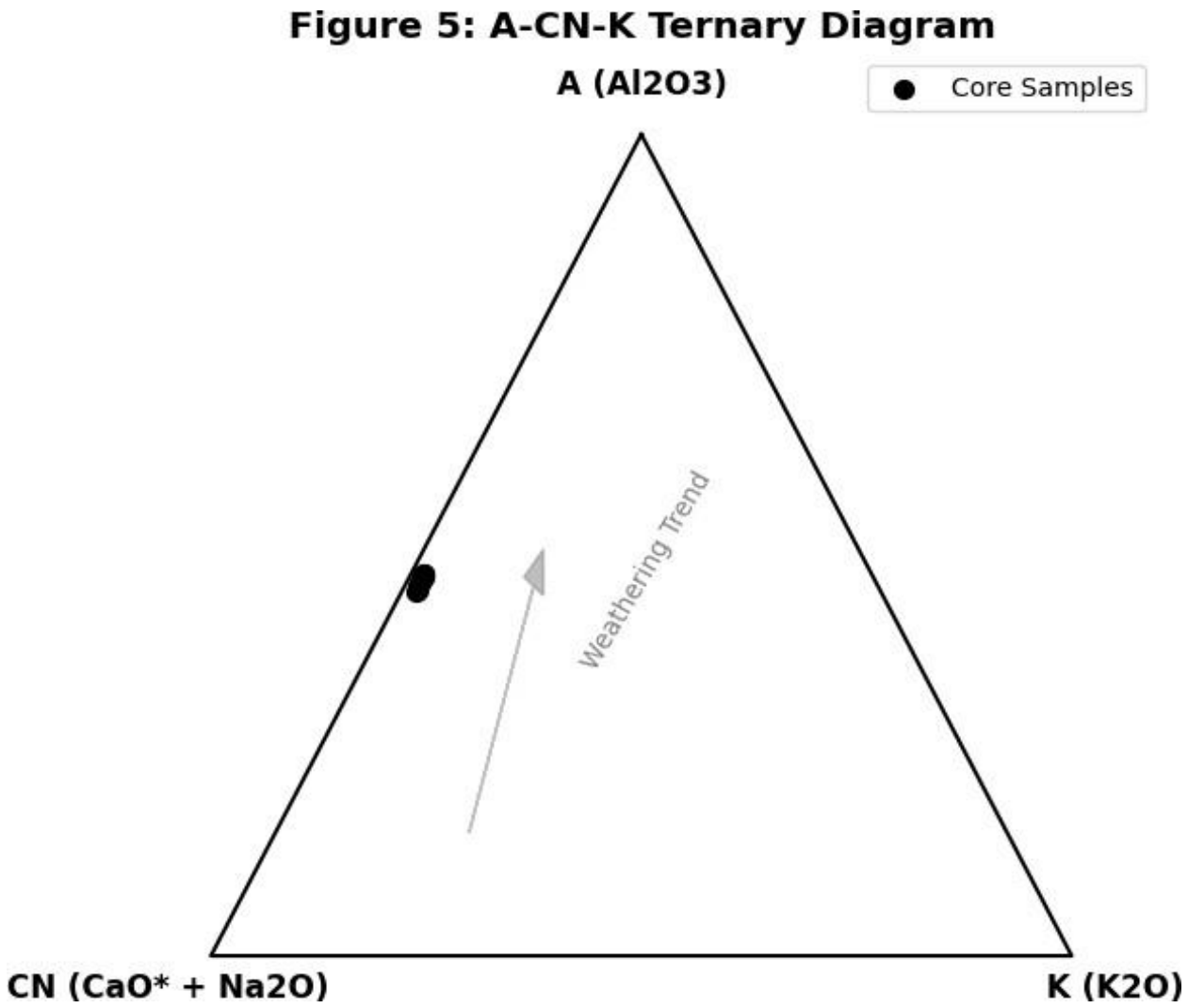

Figure 5: A-CN-K Ternary Diagram showing the clustering of all core samples along the basaltic weathering trend line, confirming a consistent source rock provenance

DISCUSSION

Paradoxical Little Ice Age Intensification

Our age model places the middle core section (L11–L19) within the Little Ice Age (LIA). While the LIA is globally associated with cooling, our geochemical data (high Al/Na, low V/Cr, high Co) indicate episodic monsoon intensification. This supports the hypothesis of regional monsoon complexity, where the Indian Summer Monsoon may have experienced wet phases despite global cooling, possibly driven by internal variability or lagged responses to North Atlantic forcing (Menzel et al., 2014; Sarkar et al., 2015).

Medieval Warm Period to Modern Transition

The core base (L1–L9), corresponding to the Medieval Warm Period, shows oxidizing conditions (higher V/Cr) and moderate productivity. The transition to the modern period (L21–L25) is marked by a return to oxidizing

conditions and significant Barium depletion, suggesting a long-term shift in lake chemistry or productivity (Tribovillard et al., 2006).

Mechanisms of Proxy Convergence

The convergence of elevated weathering (Al/Na), anoxia (low V/Cr), and productivity (high Co) in the LIA section validates the mechanism: Enhanced Monsoon →Increased Runoff →Nutrient Delivery →Productivity Surge →Bottom Water Anoxia (Algeo & Maynard, 2008).

CONCLUSIONS

High-resolution geochemical analysis of Lonar Lake sediments reveals:

1. A stable moderate weathering regime (CIA ~59) throughout the last millennium.
2. Robust evidence for episodic monsoon intensification during the Little Ice Age, challenging simple global cooling-monsoon suppression models.
3. A long-term trend of Barium depletion indicating evolving lake productivity or redox states.
4. The necessity of high-resolution local archives to resolve centennial-scale climate variability.

ACKNOWLEDGMENTS

The authors gratefully acknowledge the Wadia Institute of Himalayan Geology (WIHG) for providing analytical support for this research. Financial assistance received under the NFST Fellowship is sincerely acknowledged.

We also express our sincere gratitude to the Principal Chief Conservator of Forests (Wildlife), Amravati–Nagpur, the Chief Conservator of Forests and Field Director, Melghat Tiger Reserve, Camp Amravati, Maharashtra, and the Maharashtra State Biodiversity Board, Nagpur, for granting the necessary permissions to conduct this study.

REFERENCES

1. Algeo, T. J., & Maynard, J. B. (2008). Trace-metal covariation as a guide to water-mass conditions in ancient anoxic marine environments. Geosphere, 4(5), 872–887. https://doi.org/10.1130/GES00149.1
2. Anoop, A., Prasad, S., Basavaiah, N., Tiwari, M., & Menzel, P. (2013). Millennial-scale climate variability during the past 135 ka recorded in the sediments of the Arabian Sea: The 4.2 ka event. Quaternary International, 313–314, 114–126.
3. Armstrong-Altrin, J. S., & Verma, S. P. (2005). Geochemistry of the Jurassic and Cretaceous shales from the Scotian shelf and Kentucky, and comparison with Jurassic shales from Mexico and Peru. Chemie der Erde - Geochemistry, 65(2), 85–113.
4. Basavaiah, N., Srivastava, P., & Sharma, A. (2014). Holocene geomagnetic variations in sediments of Lonar Lake, India. Advances in Geosciences, 16, 1–10.
5. Chandran, R., Komatsu, G., & Kashyap, A. (2022). Lonar impact crater: Recent investigations and future perspectives. Current Science, 123(11), 1467–1474.
6. Dani, K. G. S., & Ramesh, R. (2015). Monsoon climate variability in ancient India: A study. Quaternary Science Reviews, 119, 184–194.
7. Fedo, C. M., Nesbitt, H. W., & Young, G. M. (1995). Unraveling the effects of potassium metasomatism on the geochemistry of granitic rocks in the Minnesota River Valley, U.S.A. Chemical Geology, 123(1–2), 59–77.
8. Fredriksson, K., Fredriksson, B. A., Balakrishna, S., et al. (1973). Lonar Lake, India: An impact crater of Holocene age. Science, 180(4092), 1063–1064.
9. Goswami, B. N., Venugopal, V., Sengupta, D., Madhusoodanan, M. S., & Xavier, P. K. (2006). Increasing trend of extreme rain events over India in a warming environment. Science, 314(5804), 1442–1445.

ISSN No. 2454-6194 | DOI: 10.51584/IJRIAS |Volume XI Issue I January 2026

10. Harnois, L. (1988). The CIW index: A new chemical index of weathering. Sedimentary Geology, 55(3–4), 319–322.
11. Komatsu, G., Abe, T., Yamazaki, A., et al. (2014). Lonar crater and lake, India: Geology, geochemistry, and paleoenvironmental change. Global and Planetary Change, 111, 179–195.
12. Menzel, P., Gaye, B., & Wiesner, M. G. (2014). Drying up of monsoonal moisture supply since the 4.2 ka event: Geochemical evidence from the Arabian Sea sediment record. Paleoceanography, 29(4), 365–380.
13. Nesbitt, H. W., & Young, G. M. (1982). Early Proterozoic climates and plate motions inferred from major element chemistry of lutites. Nature, 299(5885), 715–717.
14. Prasad, S., Kusumgar, S., Gupta, A. K., & Sharma, P. (2014). Monsoon droughts and the Indo-Pacific warm pool in the core monsoon zone of India. Quaternary Science Reviews, 103, 97–108.
15. Resmi, P. K., Unnikrishnan, A. S., Shankar, R., et al. (2022). Holocene monsoonal variations in India: Imprints on environmental records. Quaternary Science Reviews, 276, 107345.
16. Sarkar, A., Prasad, S., Swain, D. L., & Rajesh, B. (2015). Monsoon source shifts during the 4.2 ka event: Geochemical and paleomagnetic evidence from Lonar Lake, India. Quaternary Science Reviews, 128, 77–87.
17. Sinha, A., Berkelhammer, M., Stott, L., Mudelsee, M., Cheng, H., & Cai, Y. (2011). The leading mode of Indian Summer Monsoon precipitation variability during the last millennium. Geophysical Research Letters, 38, L15703.
18. Tribovillard, N., Algeo, T. J., Lyons, T., & Riboulleau, A. (2006). Trace metals as paleoredox and paleoproductivity proxies: An update. Chemical Geology, 232(1–2), 12–32.